Eastern Equatorial Pacific productivity and related-CO_2 changes since the last glacial period

Eva Calvo[a,1], Carles Pelejero[b], Leopoldo D. Pena[c], Isabel Cacho[d], and Graham A. Logan[e]

[a]Institut de Ciències del Mar, Consejo Superior de Investigaciones Científicas (CSIC), Passeig Marítim de la Barceloneta, 37-49, 08003 Barcelona, Spain; [b]Institució Catalana de Recerca i Estudis Avançats and Institut de Ciències del Mar, CSIC, Passeig Marítim de la Barceloneta, 37-49, 08003 Barcelona, Spain; [c]Lamont-Doherty Earth Observatory of Columbia University, P.O. Box 1000, Palisades, NY 10964; [d]Grup de Recerca de Geociències Marines, Departament d'Estratigrafia, Paleontologia i Geociències Marines, Universitat de Barcelona, C/Martí i Franquès, 08028 Barcelona, Spain; and [e]Geoscience Australia, General Post Office Box 378, Canberra, Australian Capital Territory 2601, Australia

Edited by John M. Hayes, Woods Hole Oceanographic Institution, Berkeley, CA, and approved February 22, 2011 (received for review July 7, 2010)

Understanding oceanic processes, both physical and biological, that control atmospheric CO_2 is vital for predicting their influence during the past and into the future. The Eastern Equatorial Pacific (EEP) is thought to have exerted a strong control over glacial/interglacial CO_2 variations through its link to circulation and nutrient-related changes in the Southern Ocean, the primary region of the world oceans where CO_2-enriched deep water is upwelled to the surface ocean and comes into contact with the atmosphere. Here we present a multiproxy record of surface ocean productivity, dust inputs, and thermocline conditions for the EEP over the last 40,000 y. This allows us to detect changes in phytoplankton productivity and composition associated with increases in equatorial upwelling intensity and influence of Si-rich waters of sub-Antarctic origin. Our evidence indicates that diatoms outcompeted coccolithophores at times when the influence of Si-rich Southern Ocean intermediate waters was greatest. This shift from calcareous to noncalcareous phytoplankton would cause a lowering in atmospheric CO_2 through a reduced carbonate pump, as hypothesized by the Silicic Acid Leakage Hypothesis. However, this change does not seem to have been crucial in controlling atmospheric CO_2, as it took place during the deglaciation, when atmospheric CO_2 concentrations had already started to rise. Instead, the concomitant intensification of Antarctic upwelling brought large quantities of deep CO_2-rich waters to the ocean surface. This process very likely dominated any biologically mediated CO_2 sequestration and probably accounts for most of the deglacial rise in atmospheric CO_2.

marine productivity | molecular biomarkers | paleoceanography

The Eastern Equatorial Pacific (EEP) cold tongue is the major oceanic source of carbon dioxide to the atmosphere, despite the fact that it supports up to 5–10% of global marine productivity (1). Nowadays, a net flux of CO_2 from the ocean to the atmosphere is generated by the upwelling of CO_2-rich deep waters, which dominates over carbon fixation by phytoplankton and export production (2). There is also a strong link between the EEP and the high latitudes of the Southern Ocean, where the formation of intermediate waters in the subantarctic region transports previously upwelled waters south of the Antarctic Polar Front to the thermocline of the tropical Pacific via the Equatorial Undercurrent (EUC) (3).

One of the most recently proposed mechanisms to explain glacial CO_2 cycles is the Silicic Acid Leakage Hypothesis (SALH) (4, 5). It advocates for a shift in phytoplankton composition in low-latitude regions during glacial times, from coccolithophores to diatoms, as a result of an increased $Si(OH)_4$ supply from the Southern Ocean. At these high latitudes, under present Fe-limited conditions, diatoms are known to silicify much more heavily, taking up to four times more Si than N (6) and using up most of the Si upwelled around Antarctica. During glacial times, the alleviation of Fe-limiting conditions leaves unused $Si(OH)_4$ that can be transported northward in Subantarctic Mode Water (SAMW), the main source of nutrients for the tropical thermocline (7), being eventually upwelled in the EEP (3) (Fig. S1). The increase in silicate availability in the EEP would favor diatom production over coccolithophores, which cannot compete with diatoms when there is enough $Si(OH)_4$ available (8–10). This causes a reduction in calcite production, affecting the $CaCO_3$ to organic carbon rain ratio to the deep ocean and ultimately, a lowering of atmospheric CO_2 of 40 to 50 ppm (5, 11). The production of organic matter and of calcium carbonate has opposing effects on surface pCO_2. While both diatoms and coccolithophores remove dissolved CO_2 during photosynthesis and C_{org} production, coccolithophores also build a calcium carbonate skeleton that releases CO_2 into the water. On the contrary, the remineralization of organic carbon at depth releases CO_2, and the dissolution of $CaCO_3$ consumes CO_2. The overall effect of these two pumps, denoted here as the rain ratio or the export ratio of $CaCO_3$ to organic carbon to the deep ocean, will dictate the influence of the biological pump in atmospheric CO_2.

However, the impact of the SALH in the EEP region may not only depend on an increased availability of $Si(OH)_4$ in surface waters of the glacial Southern Ocean. This silica excess may not be enough to guarantee its leakage to tropical thermocline waters of the EEP if it is not effectively transported by ocean circulation. Crosta et al. (12) suggested that reduced formation rates of SAMW and Antarctic Intermediate Water during glacial times would prevent the northward flow of Si-rich waters and thus inhibit the expected biological effect on phytoplankton productivity in low-latitude areas. A corollary to the original SALH (13), however, still predicts a reduction of atmospheric CO_2 associated with a shift in the phytoplankton community despite a reduction in the ventilation of glacial intermediate waters and the associated absolute $Si(OH)_4$ flux, as long as the Si:N ratio is high enough.

Until now, the available paleoceanographic data have been inconclusive about changes in the $CaCO_3$:organic carbon export ratio during glacial times in the EEP (14–18). A reason for the lack of unequivocal data is that these studies (except ref. 16) focused only on the magnitude of diatom production instead of in its relative contribution to total export production compared with coccolithophores.

In order to test whether changes in phytoplankton composition were responsible for the atmospheric CO_2 changes observed during the last transition from glacial to interglacial conditions, we studied a sediment core from the EEP, Ocean Drilling Program (ODP) site 1240 (0° 01.31′N, 86° 27.76′W; 2,921-m water depth), located at the northern flank of the Carnegie Ridge in

Author contributions: E.C., C.P., L.D.P., and I.C. designed research; E.C., C.P., and L.D.P. performed research; G.A.L. contributed new reagents/analytic tools; E.C. and C.P. analyzed data; and E.C., C.P., L.D.P., I.C., and G.A.L. wrote the paper.

The authors declare no conflict of interest.

This article is a PNAS Direct Submission.

[1]To whom correspondence should be addressed. E-mail: ecalvo@icm.cat.

This article contains supporting information online at www.pnas.org/lookup/suppl/doi:10.1073/pnas.1009761108/-/DCSupplemental.

the Panama Basin. We present a high resolution multiproxy record of surface ocean productivity and dust inputs, based on the analyses of molecular biomarkers, and also of thermocline conditions to account for changes in upwelling and the influence of subantarctic intermediate water masses.

Results and Discussion

We analyze two marine biomarkers, long-chain alkenones as tracers of past productivity of coccolithophorid algae and brassicasterol (24-methylcholesta-5,22-dien-3β-ol) as a proxy for diatom abundances (see also *Methods*). Long-chain alkanes and alcohols, terrestrial biomarkers derived from higher plants, were also analyzed as proxies for continental input (19). Previous studies based on molecular biomarkers in the southern Caribbean (20) and the subtropical South Pacific (21) illustrated the potential of these paleoceanographic tracers to reconstruct past changes in phytoplankton composition. We also compare our productivity proxies with the $\delta^{13}C$ record for the thermocline-dwelling foraminifera *Neogloboquadrina dutertrei* in core site 1240 (22) as an indicator of the influence of waters from subantarctic origin (23). A reconstruction of deep thermocline (DT) seawater $\delta^{18}O$ (DT-δ^{18}Osw), in the main core of the EUC, provides a proxy for relative salinity changes. The DT-δ^{18}Osw calculation involved the subtraction of the Mg/Ca estimated temperature effect from the $\delta^{18}O$ record measured in the same thermocline-dwelling foraminifera samples (*N. dutertrei*) and the removal of the global sea level component (24) of the seawater $\delta^{18}O$ composition. Thus, more positive values of DT-δ^{18}Osw indicate saltier waters at the thermocline, whereas more negative DT-δ^{18}Osw implies fresher waters. These positive values have also been recently ascribed to increased upwelling of EUC waters from the thermocline to the surface (22). The EUC is characterized by high-salinity waters (25), and thus saltier waters at the thermocline (higher DT-δ^{18}Osw values) can be associated with an intensified EUC and strengthened upwelling from the thermocline to the surface (22).

Today, marine productivity in the EEP is colimited by iron, due to low dust inputs, and also by the low $Si(OH)_4$ content of upwelled waters of Southern Ocean origin that bathe this area (26). Thus, past changes in productivity will reflect both changes in upwelling (intensity and/or nutrient content) and in dust inputs. In Fig. 1, we compare the two marine biomarkers, associated with diatom and coccolithophorid production, with the terrestrially derived C_{26}-alcohol record as a proxy of dust inputs (the most significant source of terrestrial material to this location) and, therefore, of iron availability. During the last glacial period, all three biomarkers showed very similar patterns, with higher abundances between 23–33 ka compared with today. Another maximum also occurs between 20 and 15 ka, during the late glacial/early deglaciation. The higher flux of eolian dust inferred from the C_{26}-alcohol record during the last glacial period is consistent with recent studies of dust deposition measuring ^{232}Th fluxes in marine cores from the central and eastern equatorial Pacific (27–29) (Fig. 1). In the EEP, high dust inputs were maintained until 15 ka (29, 30) as indicated by our C_{26}-alcohol record. After 15 ka, both alkenones and the C_{26}-alcohol records display decreasing trends toward the low values recorded during the Holocene. In contrast, the diatom marker, brassicasterol, shows a third maximum between 12.5 and 9 ka.

Our marine biomarkers do not show the expected shift between coccolithophores and diatoms predicted by the SALH during the last glacial period that could account for the lowering of atmospheric CO_2 concentrations through a reduced carbonate pump. Instead, the increase in both alkenones and brassicasterol between 23 and 33 ka may indicate a global positive response of the whole phytoplanktonic community to local fertilization by eolian dust inputs. An enhanced biological pump has also been invoked to operate in the EEP during the last glacial maximum based on a silicon isotope record (31). So far, most of

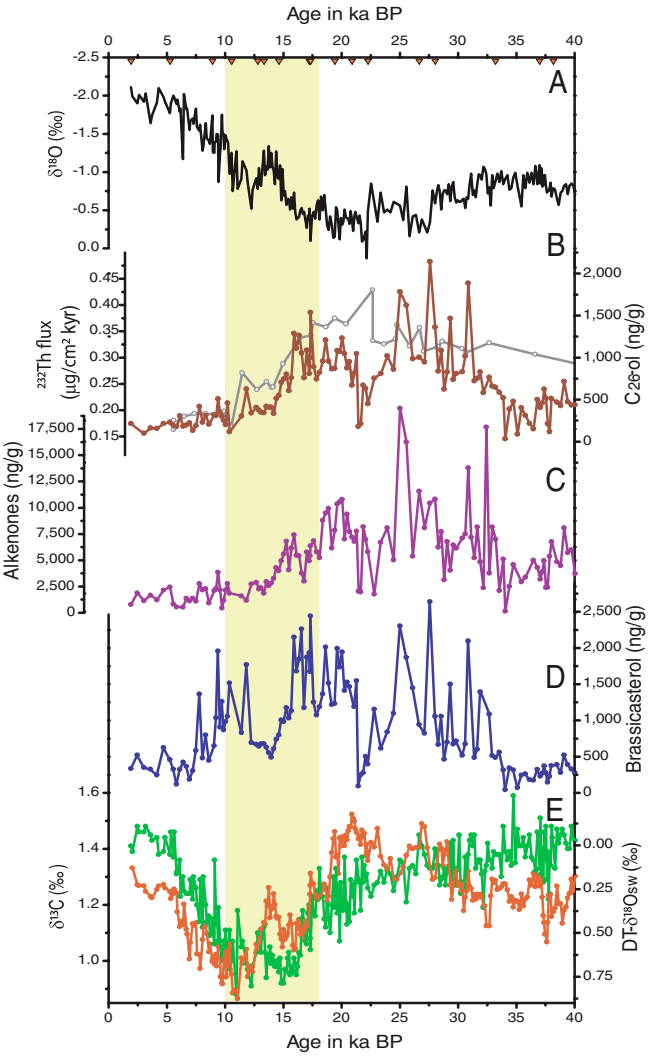

Fig. 1. Records from ODP site 1240 comparing marine productivity, dust inputs, and circulation/ventilation proxies over the last 40 ka. (*A*) $\delta^{18}O$ of planktonic foraminifera *Globigerinoides ruber* (plotted for stratigraphic purposes). (*B*) Dust inputs based on the concentration of the terrestrial biomarker C_{26} alcohol (brown line) and ^{232}Th fluxes from nearby core TTN013-PC72 (30). (*C*) Concentrations of the marine biomarker C_{37} alkenones as a proxy for coccolithophore production. (*D*) Concentrations of the marine biomarker brassicasterol as a proxy for diatom production. (*E*) $\delta^{13}C$ of the thermocline-dwelling foraminifera *N. dutertrei* (22) as an indicator of the influence of waters from subantarctic origin (green line) and deep thermocline seawater $\delta^{18}O$ (DT- δ^{18}Osw) reconstruction as a proxy for salinity changes and upwelling intensity (22). Triangles on the top axis mark AMS ^{14}C dates. Colored bar marks the last glacial/interglacial transition.

the attempts to test the SALH were based on opal records from the tropical Pacific (14, 15, 17, 18). These studies challenged the SALH on the basis of a decrease in opal accumulation during glacial times. However, they were inconclusive for two reasons. First, they did not consider changes in the carbonate pump, a requirement of the SALH (13). Second, they did not take into account that a decrease in opal accumulation may not necessarily be due to a decrease in diatom productivity but could also relate to less silicified diatoms as a consequence of the increased local iron input during glacial times (31). Overall, our biomarker records indicate that either the Southern Ocean Si excess did not reach the location of site 1240 and/or the local Fe-induced Si excess was not large enough to promote the phytoplanktonic shift during glacial times because perhaps diatom growth was somehow limited by other ecological factors. In the subantarctic

region, however, Calvo et al. (21) did find an increase in diatoms over coccolithophores in glacial sediments, suggesting the arrival of Si-rich waters, at least, to the midlatitudes of the Southern Ocean. A low diatom to coccolithophore ratio is also evident during the late Holocene (Fig. 2*A* and *Methods*), although, unlike glacial times, conditions in the Southern Ocean leading to the low

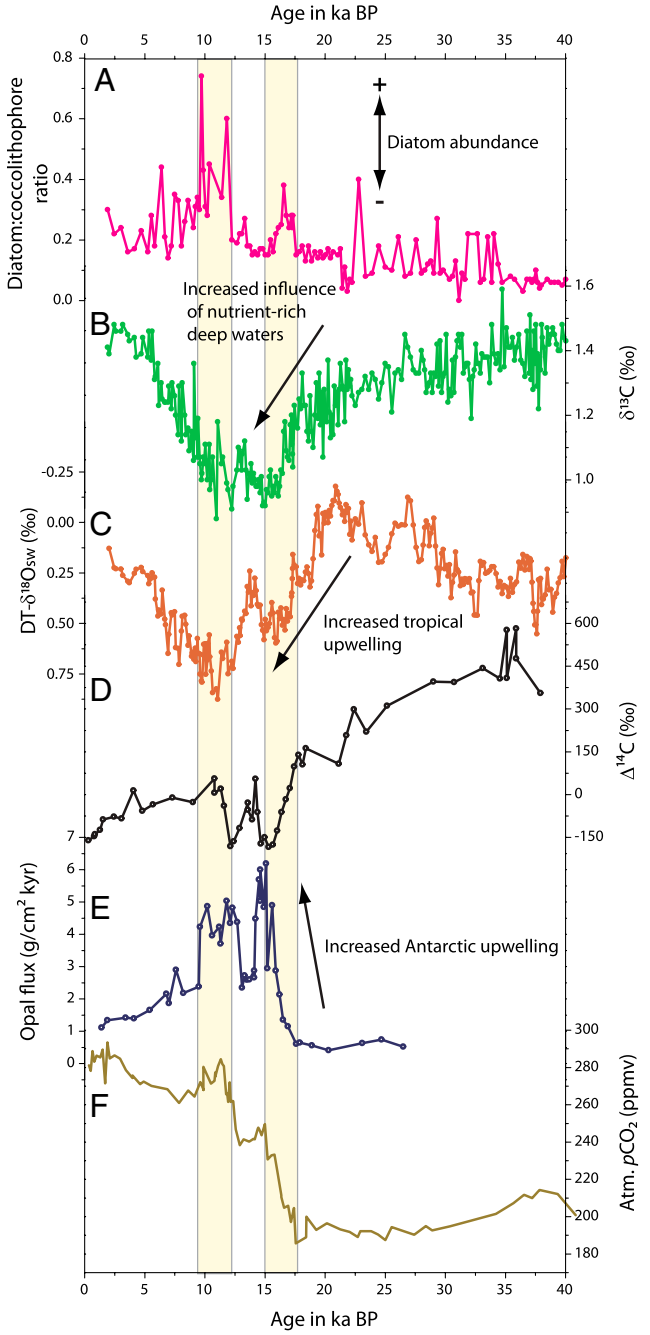

Fig. 2. Comparison of site 1240 records with other available climate records. (*A*) Brassicasterol/(Brassicasterol + C_{37} alkenones) ratio as an indicator of the relative abundance of diatoms over coccolithophores. (*B*) δ^{13}C of the thermocline-dwelling foraminifera *N. dutertrei*. (*C*) Deep thermocline seawater δ^{18}O (DT- δ^{18}Osw) reconstruction. (*D*) Intermediate-water Δ^{14}C record from Baja California as a proxy for deep ocean ventilation (37). (*E*) Opal flux from Antarctic core TN057-13PC as a proxy for upwelling in the Southern Ocean (36). (*F*) Atmospheric CO_2 concentration recorded in Antarctic ice cores (39). Colored bars represent periods of enhanced deep water ventilation (low Δ^{14}C values), resumption of Antarctic upwelling (high opal fluxes) and greater impact of high latitude waters in the thermocline waters of the EEP.

diatom productivity in the equatorial Pacific were likely different. The lower dust-derived Fe inputs to the Southern Ocean (30) and its impact on diatom Si:C uptake ratios would have left no Si available to be transported to lower latitudes.

In contrast, silica leakage does seem to have reached and affected low latitudes during the deglaciation at certain periods (17.5–15.5 ka and 12.2–9.2 ka). This is traced in our core by an increase in brassicasterol concentrations that are not paralleled by increasing alkenone production. This evidence points to higher diatom to coccolithophore production (Fig. 2*A*), which would lead to less calcite exported from surface waters and a decrease in atmospheric CO_2. At this time, our circulation proxies also show a change in the chemistry of the water masses bathing our site starting during the early deglaciation.

In Fig. 2, we present the δ^{13}C record for *N. dutertrei* in the same core (22). At site 1240, a change in the chemical properties of Southern Ocean intermediate waters is recorded as an intense negative δ^{13}C excursion starting at 17–18 ka. At the same time, the alkenone and brassicasterol records show an increase in the diatom to coccolithophore ratio (Fig. 2*A*). Spero and Lea (23) argued that these negative excursions in the *N. dutertrei* δ^{13}C records from the EEP during deglaciation were a response to the advection of a low δ^{13}C signal from aged circumpolar deep waters into the SAMW source region. However, during the last glacial period, a reduced deep water ventilation (32–34) prevented the advection of nutrient-rich/ δ^{13}C-depleted waters to the tropical thermocline, as reflected by the enriched δ^{13}C values (Fig. 2*B*) and the lower diatom to coccolithophore ratio (Fig. 2*A*). In the early deglaciation, the poleward movement of the westerlies and the retreat of sea ice (34) caused depleted δ^{13}C waters to be upwelled and incorporated in intermediate waters. These were then transported to the low latitudes of the EEP, leaving a signature in the foraminifera shells. In agreement with the negative excursion of the δ^{13}C record, the reconstruction of DT-δ^{18}Osw from the same core shows more enriched values indicative of more saline waters (Fig. 2*C*). This has recently been ascribed to increased upwelling of EUC waters from the thermocline to the surface (22). A δ^{15}N reconstruction from the same studied site also supports enhanced arrival of nutrients (increased upwelling) during the deglaciation, in agreement with maxima in the diatom to coccolithophore ratio (35).

An enhanced advection of Si-rich waters from southern origin during the deglaciation, as suggested by the prevalence of diatoms over coccolithophores at ODP site 1420, is also supported by an opal flux record from Southern Ocean sediments [Fig. 2*E* (36)]. This record shows two maxima in opal flux during the deglaciation, in synchrony with increased abundances of brassicasterol in the EEP record. The enhanced upwelling of deep waters in the Southern Ocean at the initiation of deglaciation also brought accumulated silica to surface waters, increasing opal production in this area and also allowing part of this silica to be transported to the EEP thermocline. Further evidence for the connection between the Southern Ocean and these low latitudes comes from a reconstruction of ^{14}C activities in a sediment core located at intermediate water depths off Baja California (37). The Δ^{14}C record shows two excursions of low ^{14}C activities during the last deglaciation, indicating the arrival of relatively older waters to the studied site (Fig. 2*D*). Marchitto et al. (37) related these results to the exposure of deep and isolated waters from the Southern Ocean to the atmosphere and its subsequent northward transport via intermediate waters. Moreover, direct evidence from a marine core recovered in the Atlantic sector of the Southern Ocean strongly supports the existence of a poorly ventilated deep carbon reservoir during glacial times that was subsequently released to the atmosphere during the last deglaciation (38).

Along with these old ^{14}C-depleted and Si-rich waters [reflected by the shift in phytoplankton composition in the EEP and the increased opal productivity in the Southern Ocean (36)], the

resumption of upwelling also resulted in a major CO_2 outgassing to the atmosphere, which coincides with the two-step rise in atmospheric CO_2 concentrations recorded in Antarctic ice cores (39) (Fig. 2*F*). The close link between the EEP and the high latitudes of the Southern Hemisphere is also seen between approximately 13 and 15 ka when all proxies vary in accordance. The data reflect reduced upwelling (more depleted DT-δ^{18}Osw values), slightly attenuated influence of Si-rich Southern Ocean waters (more enriched δ^{13}C values), and reduced phytoplankton productivity (lower biomarker abundances and diatom : alkenone ratios). This is in agreement with the Δ^{14}C and opal flux records and corresponds to a CO_2 plateau (Figs. 1 and 2).

Overall, the remarkable correlation between our EEP records and those from high latitudes reveals the tight link between high southern and low tropical latitudes. It is also consistent with a high latitude control on low-latitude biological productivity (7). Importantly, the expected changes in phytoplankton composition, as predicted by the SALH, that could have lowered atmospheric CO_2 concentrations did not take place during glacial times, although the dust-stimulated increase in total productivity may still have partially contributed to driving past glacial/interglacial CO_2 changes (5, 40). Instead, an increase in diatom with respect to coccolithophore productivity did occur during the deglaciation, although this floral shift, and the resulting reduction of the carbonate pump, was apparently not sufficient to counteract the return to the atmosphere of large amounts of CO_2 delivered by the oceans through an enhanced ventilation of deep southern waters.

Methods

Molecular Biomarker Analyses. ODP core 1240 was sampled every 4 cm for the upper 5.5 m for biomarker analyses and every 2 cm for C and O isotopes analyses (22). The age model was constructed from 17 Accelerator Mass Spectrometry (AMS) ^{14}C ages of monospecific samples of the planktonic foraminifera *N. dutertrei* (22).

Analysis and characterization of total lipid content were performed at Geoscience Australia laboratories following published methods (41, 42). Briefly, 0.5–2 g of freeze-dried sediment were loaded into 11-mL stainless steel extraction cells of a Dionex ASE 200 pressurized liquid extraction system. After addition of an internal standard (*n* hexatriacontane) and subsequent extraction with dichloromethane, the extracts (approximately 25 mL) were evaporated to dryness under a nitrogen stream. Six percent potassium hydroxide in methanol was used to hydrolyze wax esters and eliminate interferences during quantization of gas chromatographic data. After derivatization with bis (trimethylsilyl) trifluoroacetamide, extracts were dissolved in toluene and then injected in a Hewlett-Packard HP6890 Gas Chromatograph with a flame ionization detector and equipped with a CP-Sil 5 CB capillary column (50 m, 0.25 mm i.d., and 0.25-μm film thickness). The oven was programmed from 90 °C (holding time of 1 min) to 160 °C at 15 °C/ min, 160 °C to 280 °C at 10 °C/ min with 30-min holding time at 280 °C, and finally from 280 °C to 310 °C at 6 °C/ min with a holding time of 6 min. Selected samples were analyzed by GC-MS for compound identification, using a Hewlett-Packard HP5973 MSD attached to an HP6890 GC and with the same capillary column. The mass spectrometer was operated at 70 eV in full scan mode from 50 to 600 m/z.

Marine Productivity Proxies. Long-chain alkenones, in particular di- and tri- unsaturated C_{37} alkenones, are used here to trace back the input of Haptophyta algae, such as the coccolithophore *Emiliania huxleyi*, the most abundant source of alkenones in today's ocean waters (43). Similarly, 24-methylcholesta-5,22-dien-3β-ol (brassicasterol) has also been used as a proxy for diatom abundances (20, 21). Brassicasterol represents the major sterol in some species of diatoms (44), although a recent study suggests that this compound may be abundant only in pennate diatoms (45). Brassicasterol can also be synthesized by other microalgae, such as haptophytes and cryptophytes. In this work, we mostly focus on periods of decoupling between the alkenone and brassicasterol records, as this phenomenon implies that the sources of these biomarkers must have been different. Changes in the different contribution of coccolithophores and diatoms to brassicasterol abundances are also evaluated qualitatively looking at the brassicasterol/(brassicasterol + alkenone) ratio (Fig. 2*A*). This ratio should take higher values when diatoms predominate over coccolithophores.

Terrestrial Proxies. We use long-chain even *n* alcohols derived from terrestrial higher plants as tracers of terrestrial input to the marine environment. For simplicity, only *n* hexacosanol (*n*-C_{26}-ol), the most abundant *n*-alcohol homologue of all terrestrial *n* alcohols, is presented in this work. Another terrestrial biomarker, the long-chain *n* alkanes, was also quantified, showing the same general pattern than the long-chain *n* alcohols but with lower abundances.

The general trend of concentration estimates of the specific sedimentary compounds agrees well with ^{230}Th-normalized fluxes calculated from measurements in site 1240 (31).

ACKNOWLEDGMENTS. We thank Robert Anderson, Thomas Marchitto, and Gisela Winckler for kindly providing data. E.C., C.P., and I.C. acknowledge funding from the Spanish Ministerio de Ciencia e Innovación through Grants CTM2006-01957/MAR and CTM2009-08849/MAR, and a Ramón y Cajal Contract (to E.C.). L.D.P. acknowledges support from National Science Foundation Grant OCE-10-31198. G.A.L. published with permission of Geoscience Australia. This is a contribution from the Marine Biogeochemistry and Global Change research group, funded by Generalitat de Catalunya (Catalan Government) through Grant 2009SGR142.

1. Field CB, Behrenfeld MJ, Randerson JT, Falkowski P (1998) Primary production of the biosphere—Integrating terrestrial and oceanic components. *Science* 281:237–240.
2. Takahashi T, et al. (2009) Climatological mean and decadal change in surface ocean pCO_2, and net sea-air CO_2 flux over the global oceans. *Deep-Sea Res Pt II* 56:554–577.
3. Toggweiler JR, Dixon K, Broecker WS (1991) The Peru upwelling and the ventilation of the South Pacific thermocline. *J Geophys Res* 96:20467–20497.
4. Brzezinski MA, et al. (2002) A switch from $Si(OH)_4$ to NO_3^- depletion in the glacial Southern Ocean. *Geophys Res Lett* 29:1564, 10.1029/2001GL014349.
5. Matsumoto K, Sarmiento J, Brzezinski MA (2002) Silicic acid leakage from the Southern Ocean: A possible explanation for glacial atmospheric pCO_2. *Global Biogeochem Cy* 16:1031, 10.1029/2001GB001442.
6. Franck VM, Brzezinski MA, Coale KH, Nelson DM (2000) Iron and silicic acid concentrations regulate Si uptake north and south of the Polar Frontal Zone in the Pacific Sector of the Southern Ocean. *Deep-Sea Res Pt II* 47:3315–3338.
7. Sarmiento JL, Gruber N, Brzezinski MA, Dunne JP (2004) High-latitude controls of thermocline nutrients and low latitude biological productivity. *Nature* 427:56–60.
8. Brown CW, Yoder JA (1994) Coccolithophorid blooms in the global ocean. *J Geophys Res* 99:7467–7482.
9. Dugdale RC, Wilkerson FP (2001) Sources and fates of silicon in the ocean: The role of diatoms in the climate and glacial cycles. *Sci Mar* 65(S2):141–152.
10. Egge JK, Aksnes DL (1992) Silicate as a regulating nutrient in phytoplankton competition. *Mar Ecol-Prog Ser* 83:281–289.
11. Archer D, Winguth A, Lea DW, Mahowald N (2000) What caused the glacial/interglacial atmospheric pCO_2 cycles? *Rev Geophys* 38:159–189.
12. Crosta X, Beucher C, Pahnke K, Brzezinski MA (2007) Silicic acid leakage from the Southern Ocean: Opposing effects of nutrient uptake and oceanic circulation. *Geophys Res Lett* 34:L13601.
13. Matsumoto K, Sarmiento JL (2008) A corollary to the silicic acid leakage hypothesis. *Paleoceanography* 23:PA2203, 10.1029/2007PA001515.
14. Bradtmiller LI, Anderson RF, Fleisher MQ, Burckle LH (2006) Diatom productivity in the equatorial Pacific Ocean from the last glacial period to the present: A test of the silicic acid leakage hypothesis. *Paleoceanography* 21:PA4201, 10.1029/2006PA001282.
15. Dubois N, et al. (2010) Sedimentary opal records in the eastern equatorial Pacific: It is not all about leakage. *Global Biogeochem Cy* 24:GB4020, 10.1029/2009PA001781.
16. Higginson MJ, Altabet M (2004) Initial test of the silicic acid leakage hypothesis using sedimentary biomarkers. *Geophys Res Lett* 31:L18303, 10.1029/2004GL020511.
17. Kienast SS, Kienast M, Jaccard S, Calvert SE, Francois R (2006) Testing the silica leakage hypothesis with sedimentary opal records from the eastern equatorial Pacific over the last 150 kyrs. *Geophys Res Lett* 33:L15607, 10.1029/2006GL026651.
18. Pichat S, et al. (2004) Lower export production during glacial periods in the equatorial Pacific derived from $(^{231}Pa/^{230}Th)_{xs,0}$ measurements in deep-sea sediments. *Paleoceanography* 19:PA4023, 10.1029/2003PA000994.
19. Eglinton G, Hamilton RJ (1967) Leaf epicuticular waxes. *Science* 156:1322–1335.
20. Werne JP, Hollander DJ, Lyons TW, Peterson LC (2000) Climate-induced variations in productivity and planktonic ecosystem structure from the Younger Dryas to Holocene in the Cariaco Basin, Venezuela. *Paleoceanography* 15:19–29.
21. Calvo E, Pelejero C, Logan GA, De Deckker P (2004) Dust-induced changes in phytoplankton composition in the Tasman Sea during the last four glacial cycles. *Paleoceanography* 19:PA2020, 10.1029/2003PA000992.
22. Pena LD, Cacho I, Ferreti P, Hall MA (2008) El Niño–Southern Oscillation–like variability during glacial terminations and interlatitudinal teleconnections. *Paleoceanography* 23:PA3101, 10.1029/2008PA001620.
23. Spero HJ, Lea DW (2002) The cause of carbon isotope minimum events on glacial terminations. *Science* 296:522–525.
24. Waelbroeck C, et al. (2002) Sea-level and deep water temperature changes derived from benthic foraminifera isotopic records. *Quaternary Sci Rev* 21:295–305.
25. Lukas R (1986) The termination of the equatorial undercurrent in the eastern Pacific. *Prog Oceanogr* 16:63–90.

26. Dugdale RC, Wilkerson FP (1998) Silicate regulation of new production in the equatorial Pacific upwelling. *Nature* 391:270–273.
27. Anderson RF, Fleisher MQ, Lao Y (2006) Glacial-interglacial variability in the delivery of dust to the central equatorial Pacific Ocean. *Earth Planet Sci Lett* 242:406–414.
28. Kienast SS, Kienast M, Mix AC, Calvert SE, Francois R (2007) Thorium-230 normalized particle flux and sediment focusing in the Panama Basin region during the last 30,000 years. *Paleoceanography* 22:PA2213, 10.1029/2006PA001357.
29. McGee D, Marcantonio F, Lynch-Stieglitz J (2007) Deglacial changes in dust flux in the eastern equatorial Pacific. *Earth Planet Sci Lett* 257:215–230.
30. Winckler G, Anderson RF, Fleisher MQ, McGee D, Mahowald N (2008) Covariant glacial-interglacial dust fluxes in the equatorial Pacific and Antarctica. *Science* 320:93–96.
31. Pichevin LE, et al. (2009) Enhanced carbon pump inferred from relaxation of nutrient limitation in the glacial ocean. *Nature* 459:1114–1117.
32. François R, et al. (1997) Contribution of Southern Ocean surface-water stratification to low atmospheric CO_2 concentrations during the last glacial period. *Nature* 389:929–935.
33. Stephens BB, Keeling RF (2000) The influence of Antarctic sea ice on glacial-interglacial CO_2 variations. *Nature* 404:171–174.
34. Toggweiler JR, Russell JL, Carson SR (2006) Midlatitude westerlies, atmospheric CO_2, and climate change during the ice ages. *Paleoceanography* 21:PA2005, 10.1029/2005PA001154.
35. Robinson RS, Martinez P, Pena LD, Cacho I (2009) Nitrogen isotopic evidence for deglacial changes in nutrient supply in the eastern equatorial Pacific. *Paleoceanography* 24:PA4213, 10.1029/2008PA001702.
36. Anderson RF, et al. (2009) Wind-driven upwelling in the Southern Ocean and the deglacial rise in atmospheric CO_2. *Science* 323:1443–1448.
37. Marchitto TM, Lehman SJ, Ortiz JD, Fluckiger J, van Geen A (2007) Marine radiocarbon evidence for the mechanism of deglacial atmospheric CO_2 rise. *Science* 316:1456–1459.
38. Skinner LC, Fallon S, Waelbroeck C, Michel E, Barker S (2010) Ventilation of the deep Southern Ocean and deglacial CO_2 rise. *Science* 328:1147–1151.
39. Ahn J, et al. (2004) A record of atmospheric CO_2 during the last 40,000 years from the Siple Dome, Antarctica ice core. *J Geophys Res-Atmos* 109:D13305, 10.1029/2003JD004415.
40. Bopp L, Kohfeld KE, Le Quéré C, Aumont O (2003) Dust impact on marine biota and atmospheric CO_2 during glacial periods. *Paleoceanography* 18:1046, 10.1029/2002PA000810.
41. Calvo E, Pelejero C, Logan GA (2003) Pressurized liquid extraction of selected molecular biomarkers in deep sea sediments used as proxies in paleoceanography. *J Chromatogr A* 989:197–205.
42. Villanueva J, Pelejero C, Grimalt JO (1997) Clean-up procedures for the unbiassed estimation of C_{37}-C_{39} alkenone sea surface temperatures and terrigenous *n*-alkane inputs in paleoceanography. *J Chromatogr* 757:145–151.
43. Brassell SC (1993) Applications of biomarkers for delineating marine paleoclimatic fluctuations during the Pleistocene. *Organic Geochemistry*, eds MH Engel and SA Macko (Plenum Press, New York), pp 699–738.
44. Volkman (2003) Sterols in microorganisms. *Appl Microbiol Biotechnol* 60:495–506.
45. Rampen SW, Abbas BA, Schouten S, Sinninghe Damsté JS (2010) A comprehensive study of sterols in marine diatoms (Bacillariophyta): Implications for their use as tracers for diatom productivity. *Limnol Oceanogr*, pp:91–105.